

International Baccalaureate Diploma Program Extended Essay

Subject: Physics

Effects of airgap on an Eddy Current Braking System

Research Question:

How does changing the air gap between a permanent magnet and a non-ferrous rotating disk affect the braking time of the disk, determining the effectiveness of an eddy current braking system (ECB).

Session: May 2022

Word count: 3730

Table of Contents

INTRODUCTION:	1
INSPIRATION.....	1
RESEARCH QUESTION	1
BACKGROUND ON EDDY CURRENTS	2
<i>The right-hand rule</i>	3
GOVERNING EQUATIONS	5
EXPERIMENTAL INVESTIGATION:	9
OVERVIEW:	9
APPARATUS CONSTRUCTION:	10
<i>DC Motor construction:</i>	11
<i>Lever construction:</i>	12
PREEMPTIVE PREPARATIONS:	13
<i>Finding the tangential velocity of the disk:</i>	13
<i>Measuring other parameters:</i>	15
VIDEO ANALYSIS:	15
DATA COLLECTION PROCEDURE:	15
<i>Environmental conditions:</i>	15
<i>Air gap and number of magnets:</i>	16
<i>Determining magnetic field intensity at each air gap:</i>	17
DATA ANALYSIS:	18
ACQUIRED DATA:	20
OBSERVATIONS:.....	22
OBSERVATIONS:	25

EVALUATION OF PROCEDURE AND RESULTS	25
EVALUATION OF APPARATUS:	28
EVALUATION OF RESULTS:	30
<i>The skin effect:</i>	30
<i>Human error and external forces</i>	31
CONCLUSION:	31
AREAS OF FURTHER RESEARCH INCLUDE:	32
BIBLIOGRAPHY	33
APPENDIX:	35
LINEARIZED GRAPHS	36

Introduction:

With the growing need for safe and green transportation, many have turned away from the traditional mechanical braking and instead started to experiment with alternatives. The Eddy current braking system (ECB) is a frictionless system that utilizes the magnetic damping caused by eddy currents and applies it in various scientific and application fields. High speed trains, such as Shanghai's Transrapid and Japan's Chuo Shinkansen, prefers ECB systems as they produce less noise and air pollution and are more efficient.

The performance of an ECB system is dependent on a few different parameters with the most significant ones being the electrical resistivity of the conductor, the thickness of the conductor, the velocity of the conductor's motion or the magnet's motion, and the magnetic field intensity.

Inspiration

I was first exposed to the phenomenon of eddy currents when I read about the experiment where you drop a magnet through a copper tube. However, what intrigued me was the varied practical applications of an eddy current braking system and how it can aid or even replace our standard method of braking. I particularly wanted to gain a better understanding of the limitations of this phenomenon.

Research question

This experiment is concerned with how changing the air gap between a permanent magnet and a non-ferrous rotating disk affects the braking time of the disk, determining the effectiveness of an

eddy current braking system (ECB). Effectiveness in this study refers to the ECB being able to stop motion in the shortest amount of time¹.

Background on eddy currents

Named after circular eddies found on the surface of water, Eddy currents are circulating currents that are induced in a conductor (such as in a non-ferrous metal disk) when the conductor a change in magnetic flux. This change can be caused by moving a conductor in a stationary magnetic field, or by moving a magnetic field through a conductor. Lenz's Law states that currents are set up in such a way so that the magnetic field the current produces opposes the motion of the conductor, meaning the currents flow on a plane perpendicular to the magnetic field that produces it.

When a rotating disk moves in a magnetic field, created by either a permeant or electromagnet, eddy currents are produced in the conductor, opposing the magnetic field creating it. The eddy currents set up their own magnetic field, which interacts with the magnetic field of the magnets. The interaction of these two magnetic fields creates a force known as Eddy Current force.

1. Shi, Skyler. "(PDF) Investigating the Optimality of a Rotational Eddy Current Brake through Experiments." *ResearchGate*, Unknown, 1 Mar. 2016,

The right-hand rule

The right-hand rule helps determine the direction of the magnetic field when the direction of the current is known and vice versa.

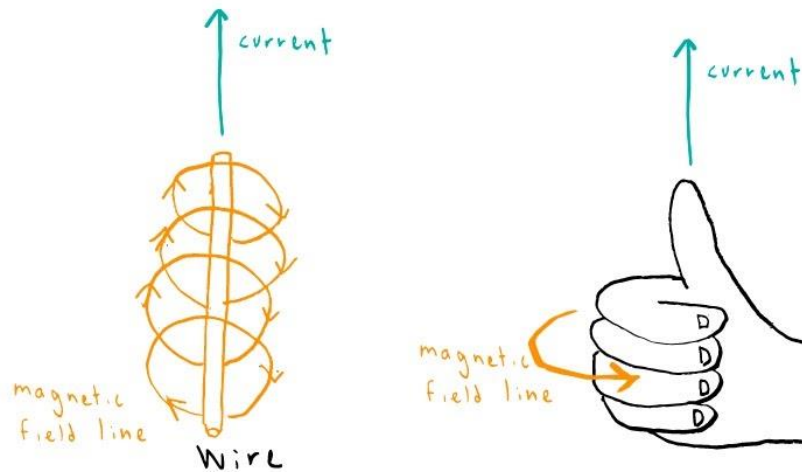


Fig. 1 Direction of induced current

Source: (<https://www.khanacademy.org/test-prep/mcat/physical-processes/magnetism-mcat/a/using-the-right-hand-rule>)

In Fig. 1, the left side shows the magnetic field lines around a wire and the direction of induced current. The right side show how the right-hand rule can be utilized. The way the fingers curl represents the way the magnetic field wraps around a wire while the thumb represents the direction of the induced current.

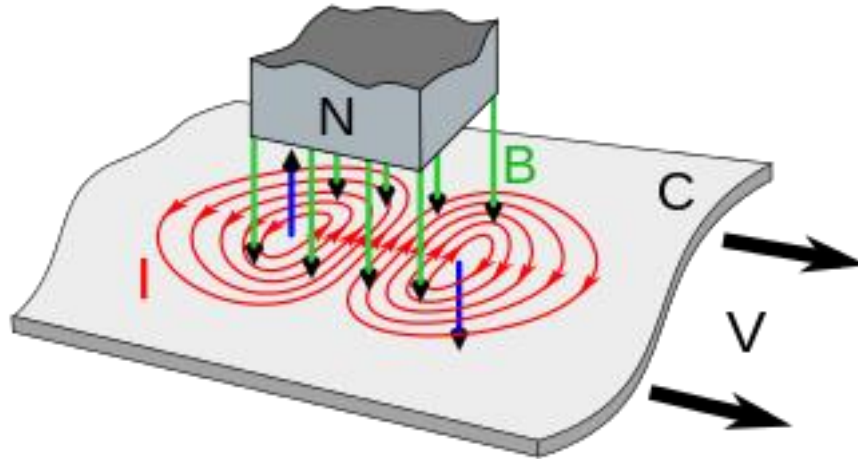


Fig. 2 Metal sheet, c , moving under stationary magnet, N

Source: (<https://imgbin.com/png/GDuX8vQG/eddy-current-brake-electrical-conductor-craft-magnets-png>)

In this diagram, c is the metal sheet moving under a stationary magnet, N . V is the velocity of the metal sheet. The magnetic field, B , passes downwards through the sheet and induces eddy currents, I . On the left side, the sheet is moving closer to the magnetic field and as a result, the magnetic flux through a given point on the sheet increases. Observing Faraday's law, $\frac{\Delta\Phi_B}{\Delta t}$ would be greater than 0 and the eddy current would be set up in the counterclockwise direction. Using the right-hand rule, one can determine the direction of the induced magnetic field points upwards in the opposite direction of the original magnetic field, creating a repulsive force.

On the right side, the sheet is moving away from the magnetic field and as a result, the magnetic flux is decreasing. Looking at Faraday's law once again, $\frac{\Delta\Phi_B}{\Delta t}$ would be less than 0 and the second eddy current would be set up in the clockwise direction. Using the right-hand rule, one can determine the direction of the induced magnetic field pointing downwards in the same direction of the original magnetic field, creating an attractive force.

What should be noted is that both the repulsive and attractive force opposes the motion of the sheet: the force tries to repulse the sheet as it comes closer to the magnet and tries to attract the disc as it moves away. These two forces combined creates the magnetic dampening effect of eddy currents. The repulsive and attractive force is the basis to an eddy current braking system.

ECB systems can be categorized into two types: linear and rotational. Depending on the need, linear or rotational ECB may be preferred over the other. Trains and roller coasters often use linear ECB while circular saws and rotational tools use rotational ECB. The underlying workings of both systems are the same. This study focuses on rotational ECB.

Governing equations

Many studies developed derived their own equations to calculate the Eddy current force. Some equations are similar and revolve around the same parameters. However, there is not one standardized way to calculate the force. Eq. 1 is from A Parametric Analysis of Magnetic Braking² by Shivanshu Shrivastava and it can be used when the conductor is moving under low speeds.

2. Shrivastava, Er. Shivanshu. “[PDF] a Parametric Analysis of Magnetic Braking the Eddy Current Brakes for High Speedand Power Automobiles and Locomotivesusing Simulink: Semantic Scholar.” *Undefined*, 1 Jan. 1970,

$$\text{Eq. 1 } F_e = \frac{1}{4\rho} \pi l^2 T B_0^2 c v$$

Where,

F_e is eddy current force (N)

ρ is the resistivity of the disk (Ω)

l is the length of the magnet (m)

T is the thickness of the disk (m)

B_0 is the magnetic field intensity (T)

c is the proportionality factor (unitless)

v is the tangential speed of the disk (ms^{-1})

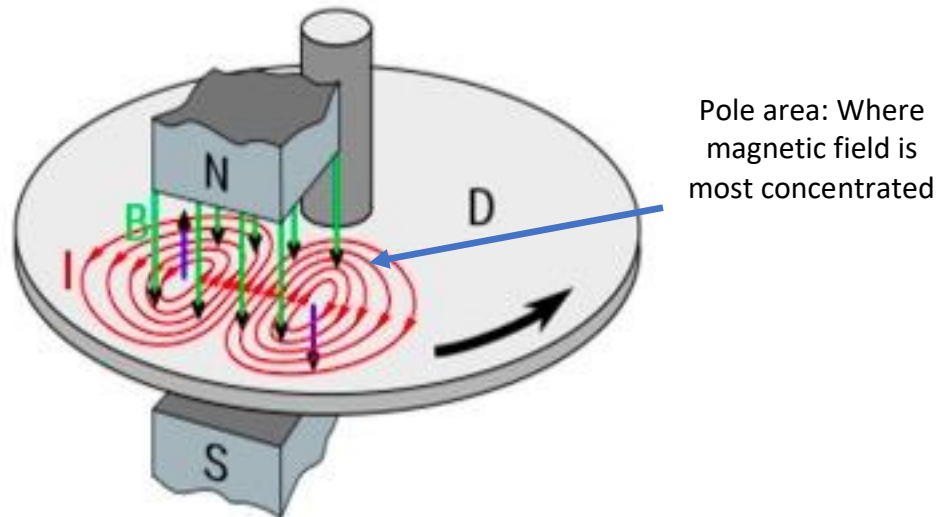


Fig. 3 Pole area

Source: (<https://imgbin.com/png/GDuX8vQG/eddy-current-brake-electrical-conductor-craft-magnets-png>)

c , the proportionality factor, is the ratio of the total amount of resistance in the disk to the amount of resistance in the pole area. It is used to account for the effects due to skin effect (later discussed) Eq. 2 shows how c can be calculated:

$$\text{Eq. 2 } c = 1 - \frac{1}{4\left(1 + \frac{r}{A}\right)^2 \left(\frac{A-r}{l}\right)^2}$$

Where,

r is the distance from the centre of the magnet to the centre of the disk

A is the radius of the disk (m)

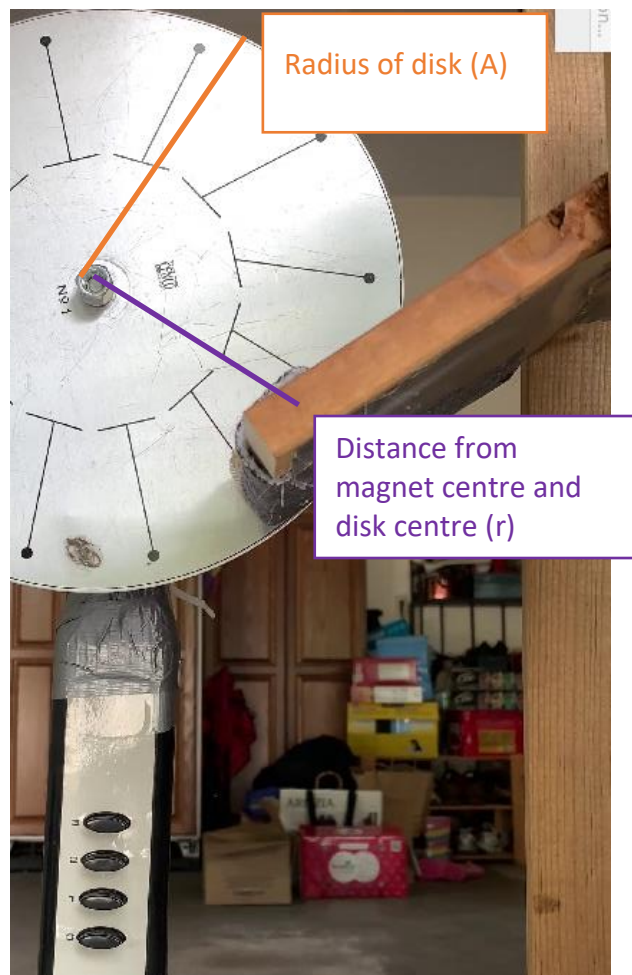


Fig 4. Radius of Disk and Distance from Magnet Centre to Disk Centre

Braking torque:

The braking torque is essentially the “power of the braking system”³. The amount of braking torque in an ECB system is directly proportional to the eddy current force. Two basic expressions (Eq. 3 and Eq. 4) for the braking torque (τ) are shown below:

$$\text{Eq. 3 } \tau = -F_e \times A$$

$$\text{Eq. 4 } \tau = I a$$

Where,

I is the moment of inertia of the disk

a is the angular acceleration of the disk

Calculating moment of inertia:

$$\text{Eq. 5 } I = \frac{L}{\omega} = \frac{mvr}{\frac{v}{A}} = mA^2$$

Where,

L is angular momentum of the disk

ω is angular velocity of the disk

m is the mass of the disk

Calculating angular acceleration:

$$\text{Eq. 6 } a = \frac{a_l}{A} = \frac{(v_f - v)}{\Delta t \times A}$$

Where,

a_l is linear acceleration

v_f is the final linear velocity of the disk $v_f = 0 \text{ ms}^{-1}$ in this experiment

Δt is the braking time

3. “What Is Brake Torque?” *What Is Brake Torque? | Race Technologies | Brembo Official*

Partner,

Plugging in Eq. 5 and Eq. 6 into Eq. 4 results in the following relationship:

$$\text{Eq. 7 } \tau = mA^2 \times \frac{-v}{\Delta t \times A} = \frac{-vmA}{\Delta t}$$

Thus, equating Eq. 7 with Eq. 3, the following relationship

$$-F_e \times A = \frac{-vm}{\Delta t}$$

$$\frac{1}{4\rho} \pi l^2 T B_0^2 c v = \frac{vm}{\Delta t}$$

$$\Delta t = \frac{4\rho m}{\pi l^2 T B_0^2 c}$$

$$\text{Eq.8 } \Delta t = \frac{4\rho m}{\pi l^2 T c} \times B_0^{-2}$$

As shown in equation Eq. 8, the magnetic field intensity (B_0) has an inverse square relationship with the braking time. The magnetic field intensity at each air gap will be experimentally determined using a magnetic field sensor. Plotting the braking time against magnetic field intensity should theoretically result in an inverse square function.

Experimental investigation:

Overview:

In this investigation, an aluminum metal disk is attached to a DC motor and is spun at a constant velocity. Permanent magnets are brought to a certain distance away from the disk as the DC motor is turned off. The shaft of the motor, where the disk is attached, continues to spin, but then the eddy currents induced in the disk quickly dampens the spinning motion and brings the disk to a stop. A video analysis program is then used to analyze the braking time with varied air gap.

Apparatus construction:

In this experiment, there are two main parts: first being the rotating disk and second being the permanent magnets the disk interacts with.

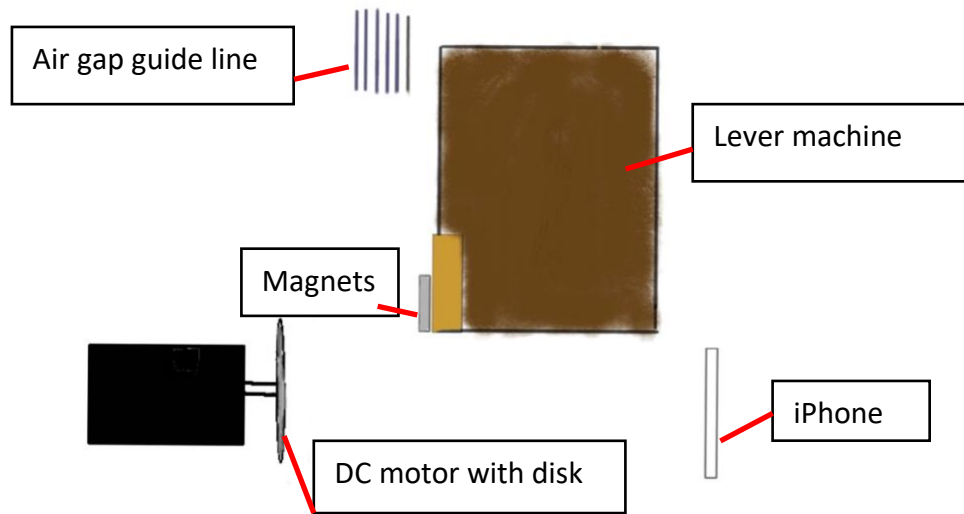


Fig 5. Sketch of full setup



Fig. 6 Full setup

DC Motor construction:

The rotating disk needs to be attached to a dc motor that can be turned on and off and when the motor is turned off the shaft, with the rotating disk, needs to continue to spin. An old mechanical fan was taken apart and striped down to just the dc motor, the stand, and the power switch. Duct tape and zip ties were used to secure the motor in place. Two nuts were used to connect the disk onto the shaft of the motor. The stand was then taped down onto the floor close to a power source. (Fig. 7)

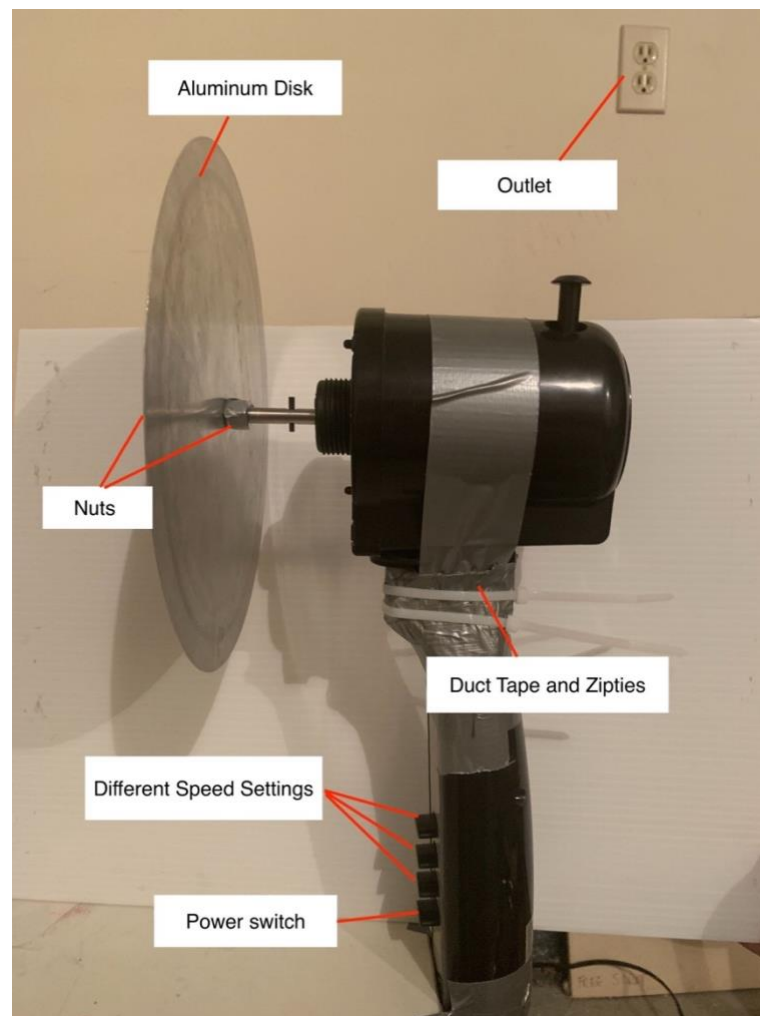


Fig. 7 Non-ferrous disk attached to dc motor

Lever construction:

The rotating disk cannot interact with the magnet until the motor is completely turned off or the eddy current will already have started dampening the motion of the disk and the disk's initial velocity would not be constant. The magnets were attached to a piece of plywood, which was then mounted onto a simple lever system made out of cedar wood. Felt fabric was inserted between the plywood and lever to stabilize the magnets. (Fig. 8)

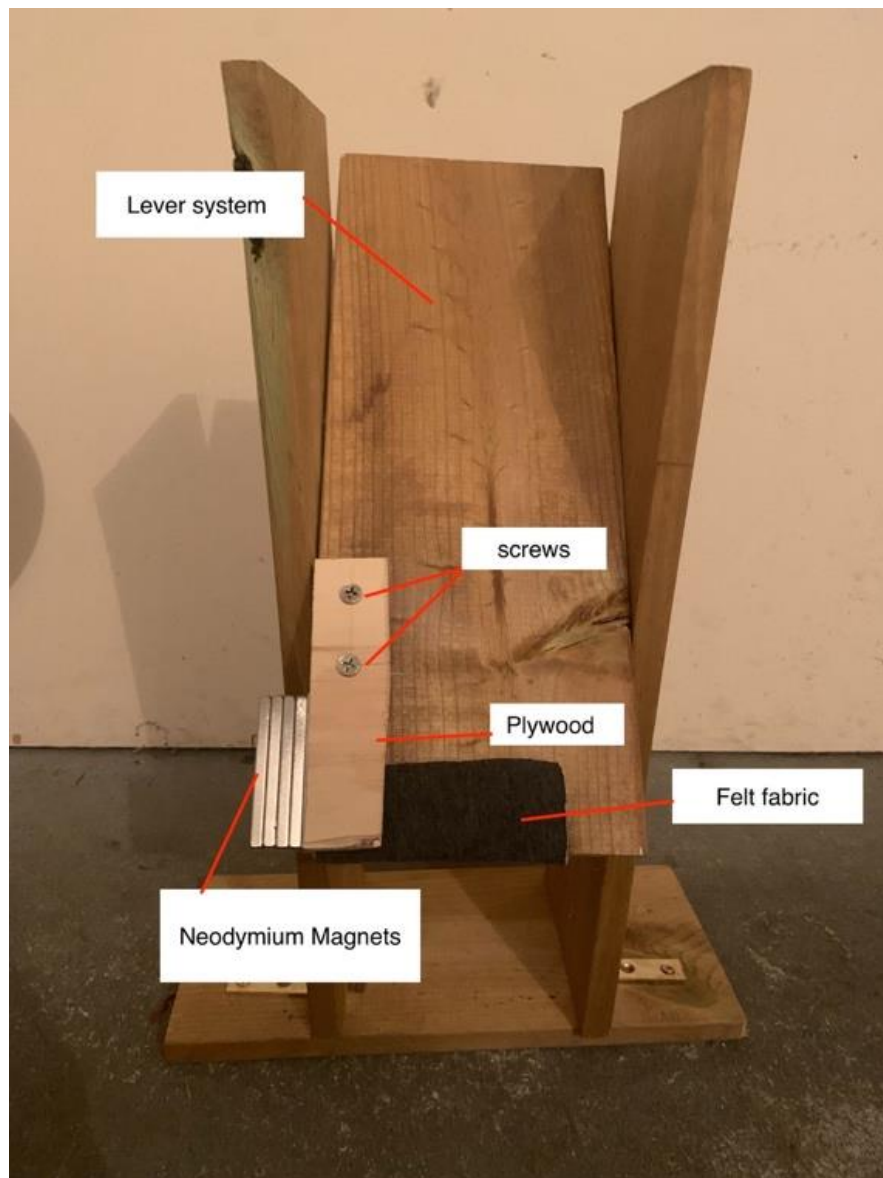


Fig. 8 Magnet lever system

The lever system was utilized so that the magnets could be kept out of the disk's proximity (Fig.9) when the motor was on and could be brought within the disk's proximity when the motor was turned off (Fig. 10).



Fig. 9 magnets out of proximity of disk



Fig.10 magnets brought within proximity of disk

Preemptive preparations:

Finding the tangential velocity of the disk:

With the motor on, the disk spins at a velocity too fast to be detectable by video analysis. To determine the initial velocity of the disk, the Magnetometer from the phyphox phone app and a small magnet was used. The small magnet, which was light enough to not alter the torque of the disk in a significant way, was placed on the edge of the disk. (Fig. 11)

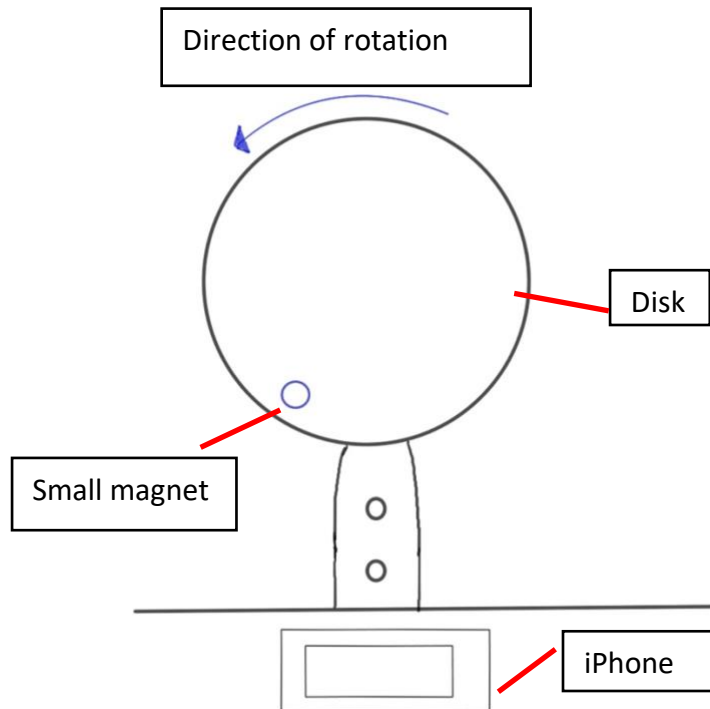


Fig. 11 phyphox and small magnet

The Magnetometer was then used to measure the time taken for one complete rotation, in $rad\ s^{-1}$. The time take for 1 complete rotation is 0.402s.

Calculating angular velocity (ω):

$$\omega = \frac{\Delta\theta}{\Delta t}$$

Where,

ω is the angular velocity of the disk ($rad\ s^{-1}$)

$\Delta\theta$ is the change in angular rotation, (rad)

Δt is the change in time (s)

$$\omega = \frac{2\pi}{0.402s} = 15.6\ rad\ s^{-1}$$

Calculating tangential velocity:

$$v = \omega r$$

$$\text{Thus, } v = 15.6 \times 0.109 = 1.7004\ ms^{-1}$$

Measuring other parameters:

The resistivity of the aluminum plate was found to be $2.82 \times 10^{-8} \Omega$. Other parameters (the length of the magnet, thickness of the disk, the distance between the centre of the magnet and the centre of the disk, and the radius of the disk) was all measured using a ruler. These values are later used to calculate the theoretical braking time of the disk at each air gap.

ρ / Ω	l / m	t / m	v / ms^{-1}	r / m	A / m	m / kg
2.82×10^{-8}	5.9×10^{-2}	4.0×10^{-4}	1.70	1.09×10^{-1}	2.53×10^{-1}	9.8×10^{-2}

Video analysis:

An iPhone 11 with a frame rate of 60 frames per second and 4k resolution was used to record the spinning disk as it interacted with the magnet. A tripod was used to secure the video recorder at an optimal position. The video was transferred to Tracker, a video analysis program, to determine the time it took the disk to stop spinning after coming in contact with the magnets.

Data collection procedure:

Environmental conditions:

The experiment was conducted in a garage where a 4m by 5m area was cleared out. During experimentations, the garage door was shut to minimize wind and to create a more isolated system.

Air gap and number of magnets:

The dc motor with the attached disk and the table where the experiment took place were both secured into position using weights and heavy-duty tape. The different air gap measurements were marked on a sheet of paper and secure onto the table with tape. The air gaps chosen ranged from 0.018m (1.80 cm) to 0.03m (3.00 cm) and incrementally increased by 0.002m (0.2cm), resulting in 10 different air gaps. The air gaps chosen were based on air gaps found in previous works and on preliminary testing. Most other research on this topic used 1mm or even smaller air gap increments.⁴ In this experiment, however, the air gap increments were not able to be as precise as previous works due to measuring device limitations. As a result, 0.002m was chosen to be the increment increased. The experiment was conducted using 6 5.9 cm by 0.95 cm by 0.45 cm neodymium magnets.



Fig. 12 Air gap guide lines

4. Chavan, Sneha, et al. "Design and Fabrication of Eddy Current Braking System." *JETIR*, JETIR(Www.jetir.org), <https://www.jetir.org/view?paper=JETIRBB06179>.

Video recording:

To start the procedure, the lever with attached magnets was aligned with the first air gap mark and the magnets were set to a position where it did not interact with the disk. The dc motor was then turned on to the first and slowest setting and the disk spun at constant velocity for a few seconds. Simultaneously, the motor shut off and the magnets were raised to interact with the disk. The trial concluded when the disk completely stopped rotating. The lever would be reset to its previous position, out of the proximity of the disk, and another trail would be run. 3 trials were conducted at each air gap.

Determining magnetic field intensity at each air gap:

Using a magnetic field sensor, the magnetic field intensity was found at each air gap. (Fig. 13)

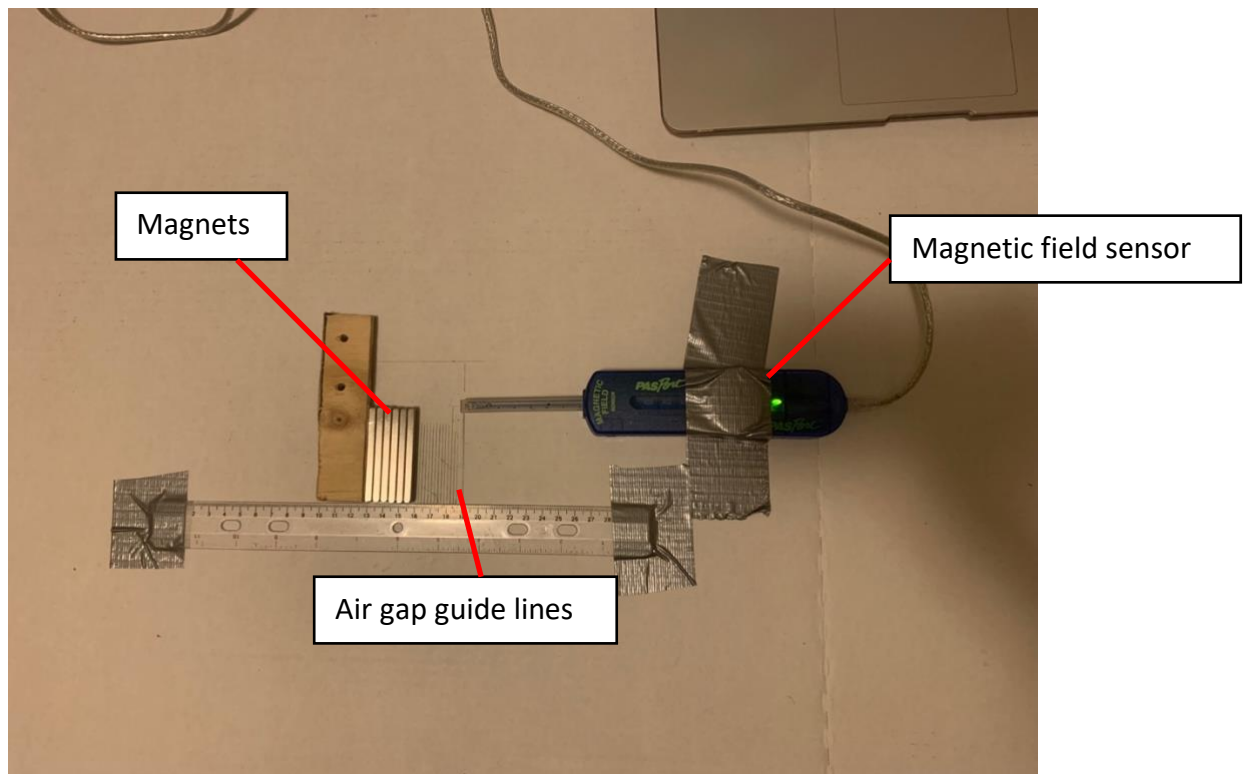
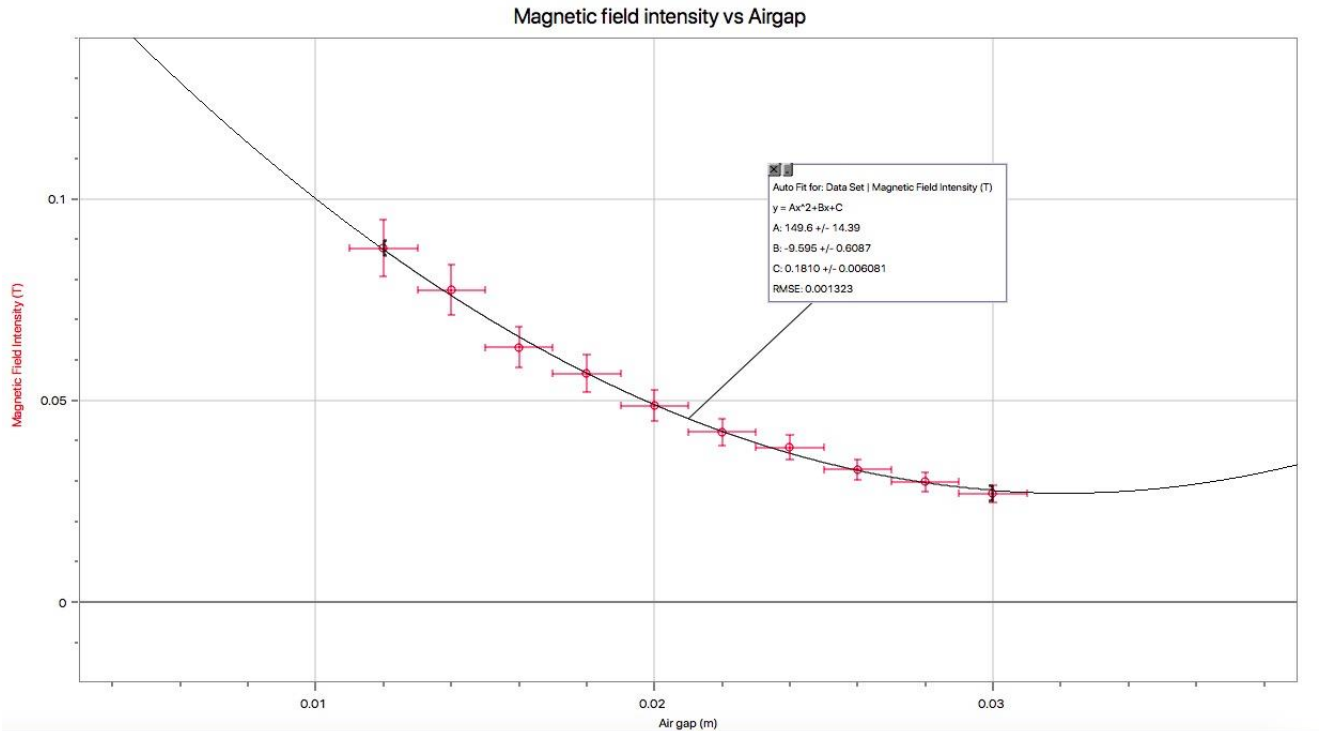


Fig. 13 Collecting Magnetic Field Strength data



Graph 1 Magnetic field intensity vs Air gap

The graph of magnetic field strength vs air gap shows a quadratic relationship between the two variables. This quadratic relationship aligns with results of previous studies⁵. The magnetic field strength at each air gap was then plotted against braking time at the corresponding air gap.

Data analysis:

In the Tracker program, the video recordings were slowed down to 10 frames per second, which allowed user to accurately mark the start time (Fig. 14), when the magnet started interacting with the disk, and the end time (Fig. 15), when the disk came to a complete stop. Using a distance and time table to track the data, the difference between start time and end time can be determined.

5. Oldenburg, Curtis M., et al. "Figure 5. Calculated and Measured Values of Magnetic Field Strength..." *ResearchGate*, 15 Oct. 2020,

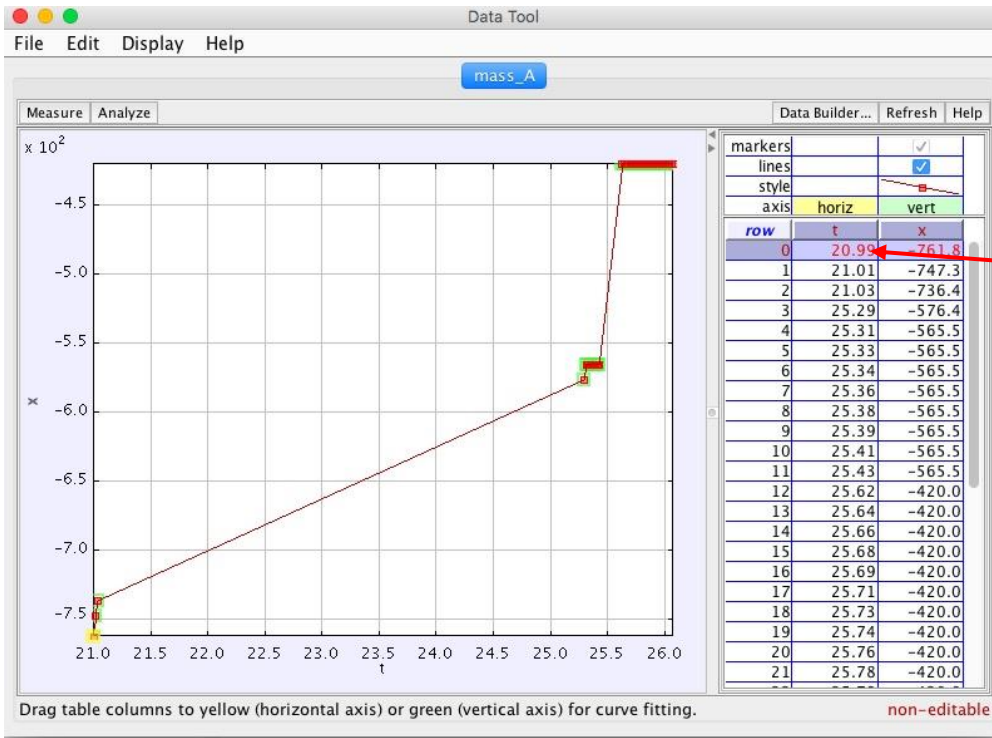


Fig. 14 Start time on Distance and Time table

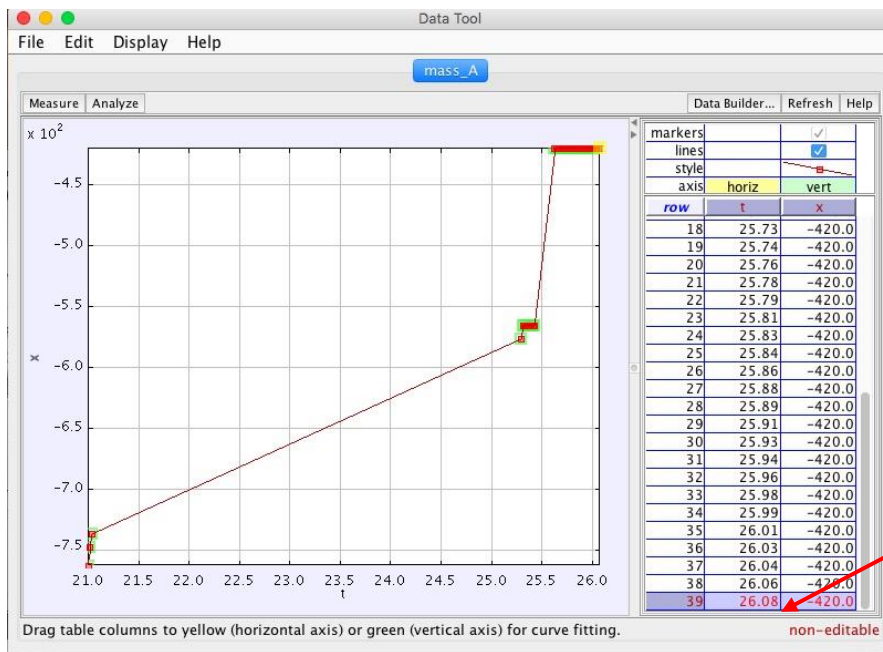


Fig. 15 End time on Distance and Time table

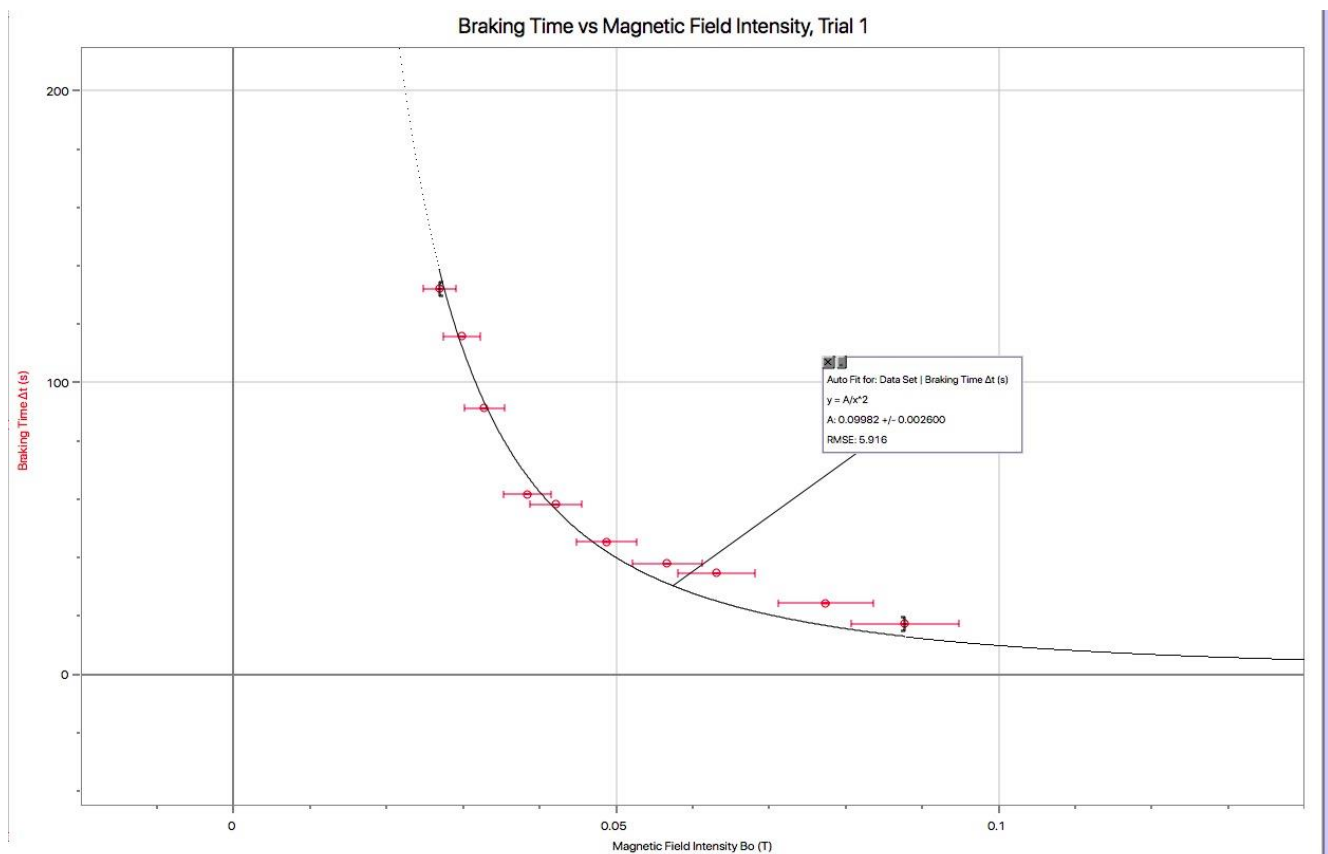
Acquired data:

Three trials were conducted at each air gap and the braking times of the disk are shown in the following tables:

Table 1 Air gap, Magnetic Field Intensity, and braking time measurements

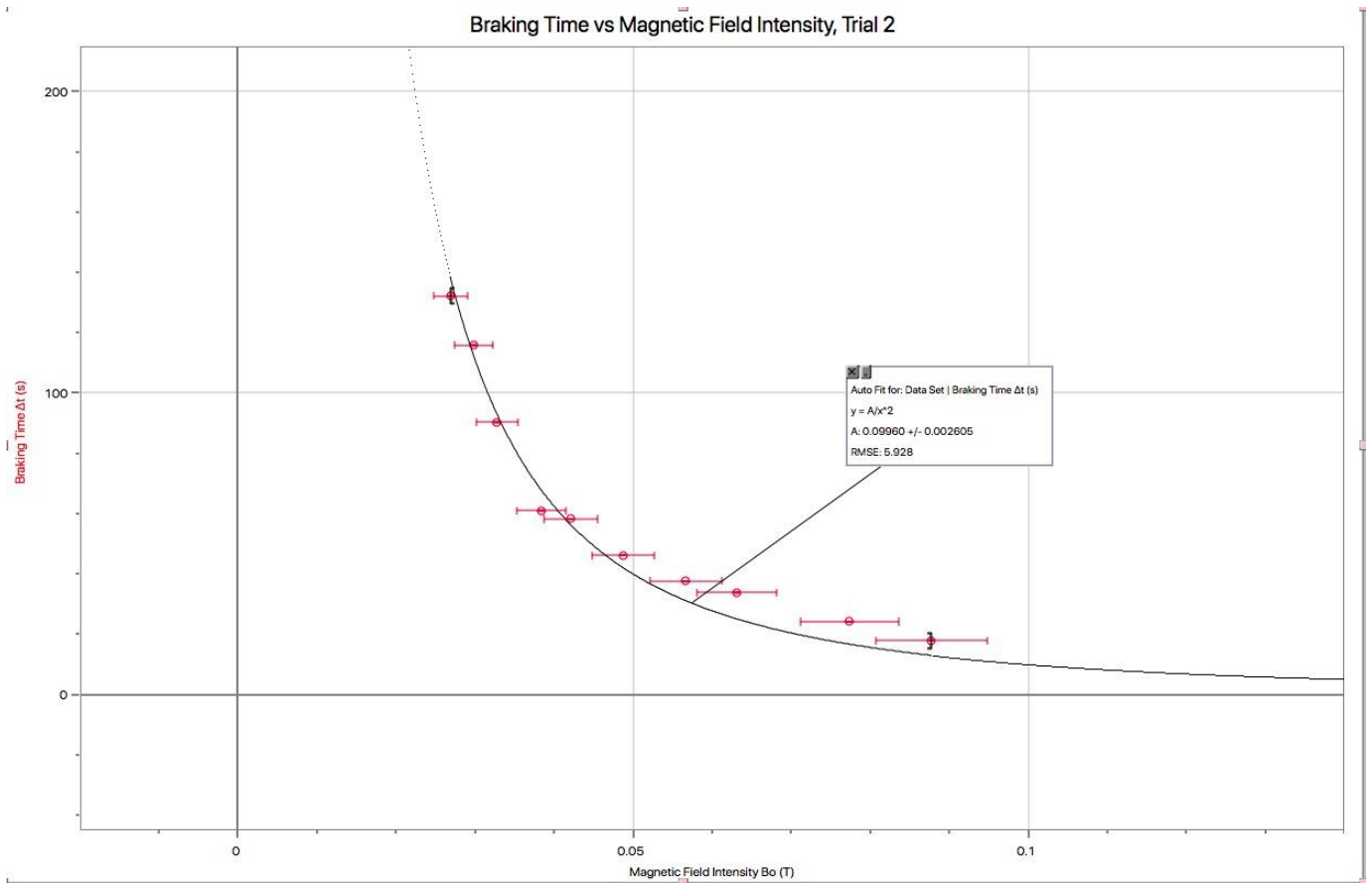
Air gap (d)/ m $\pm 0.001\text{m}$	Magnetic field intensity (B_0)/ T $\pm 10\%$ of reading	Braking time (Δt)/s $\pm 0.5\text{s}$			
		Trial 1	Trial 2	Trial 3	Average braking time
0.012	0.088	17.3	17.8	17.5	17.5
0.014	0.077	24.3	24.1	24.6	24.3
0.016	0.063	34.6	33.7	31.5	33.3
0.018	0.057	37.9	37.6	38.3	37.9
0.020	0.049	45.3	46.1	48.2	46.5
0.022	0.042	58.2	58.1	57.4	57.9
0.024	0.038	61.7	60.9	60.3	61.0
0.026	0.033	91.2	90.2	90.3	90.6
0.028	0.030	115.7	115.9	114.7	115.4
0.030	0.027	132.1	132.2	132.5	132.3

Graph 2 Braking time vs Magnetic Field Strength Trial 1

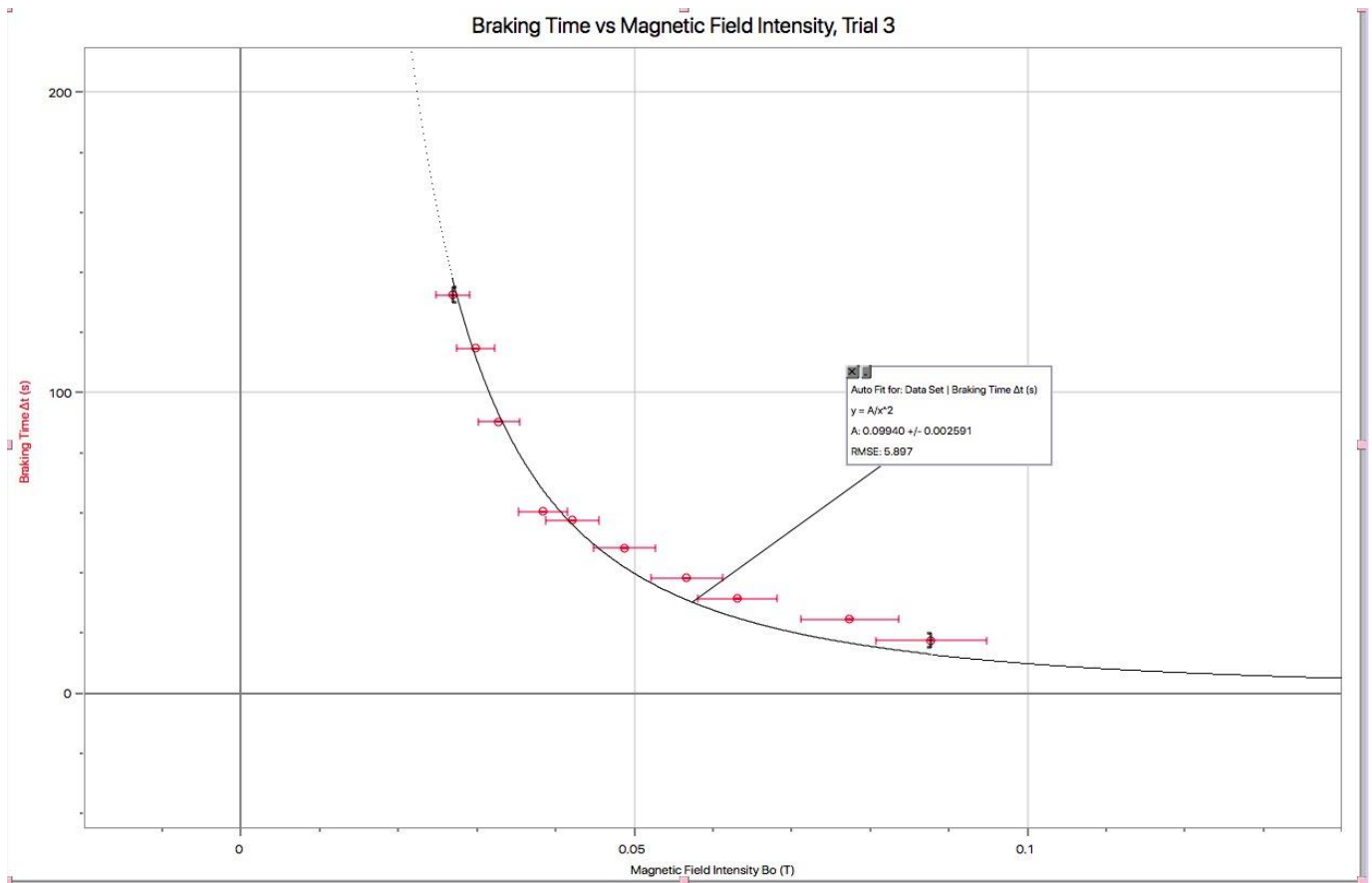


The uncertainty of the braking time is 0.5s, which is equal to half the time interval between the frames.

The uncertainty of the magnetic field intensity was 10% of reading. For example, the uncertainty for a reading of 0.088T would be 0.008 T



Graph 3 Braking time vs Magnetic Field Strength Trial 2



Graph 4 Braking time vs Magnetic Field Strength Trial

Observations:

Each magnetic field strength value corresponds to an air gap. The smallest value of magnetic field gap, 0.027 T, corresponds to the air gap 0.030 m. From first observations, it is evident that as the magnetic field increases, meaning when the air gap is smaller, the braking time decreases. The steepest slope in the graph represents the greatest change in braking time and is observed in the beginning when the air gap is still rather big.

All trials showed to have an inverse squared equation governed by $\Delta t = \frac{A}{B_0^2}$. The equation $\Delta t = \frac{A}{B_0^2}$ is governed by many parameters including the initial velocity of the disk: the mass of the disk, the radius of the disk, the resistivity of the disk, just to name a few.

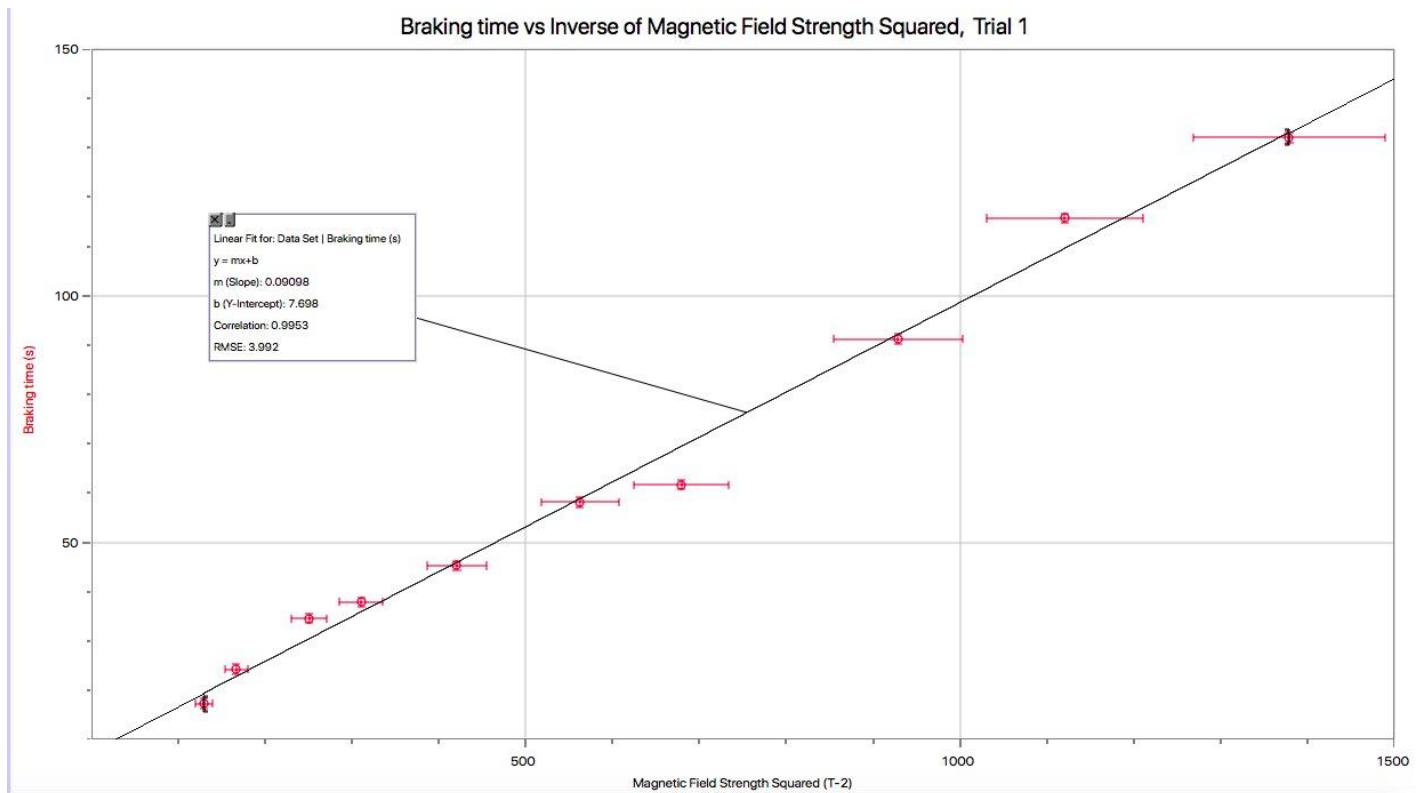
It has to be acknowledged no best-fit line in any of the graph intercepted all data points. The best-fit line started to diverge around essentially at the same air gap, at 0.018m and smaller airgaps. This suggests that a systematic error occurred at these smaller air gaps. The possible errors are either connected with the magnetic field strength or the braking time. As the magnetic field strength variables fit the best-fit curve rather well in graph 1 and fits the results of previous studies, the systematic error is most likely to do with the braking time of the disk rather than the magnetic field strength value.

Due to the large number of outliers on the graph and the large RSME, the actual relationship between the variables were inconclusive. A general relationship can be found, but the data points, especially those at a smaller air gap, diverged from the best-curve line significantly. Graph 2, 3, and 4 were linearized by plotting Δt . Linearized Graph 2 results in Graph 5. The linearized graphs of 3 and 4 can be found in the appendix. Theoretically, the relationship between Δt and B_0^{-2} should be proportional.

Table 2 Air gap, Braking time, Inverse of Magnetic Field Strength Squared

Air gap (d)/ m $\pm 0.001\text{m}$	Inverse of Magnetic Field Strength Squared (B_0^{-2}) / T $\pm 10\%$ of reading	Braking time (Δt)/s $\pm 0.5\text{s}$			
		Trial 1	Trial 2	Trial 3	Average braking time
0.012	129.87	17.3	17.8	17.5	17.5
0.014	166.90	24.3	24.1	24.6	24.3
0.016	250.97	34.6	33.7	31.5	33.3
0.018	311.14	37.9	37.6	38.3	37.9
0.020	421.07	45.3	46.1	48.2	46.5
0.022	562.68	58.2	58.1	57.4	57.9
0.024	679.30	61.7	60.9	60.3	61.0
0.026	928.60	91.2	90.2	90.3	90.6
0.028	1120.65	115.7	115.9	114.7	115.4
0.030	1378.99	132.1	132.2	132.5	132.3

Graph 5 Braking time vs Inverse of Magnetic Field Strength Squared, Trial 1



Observations:

After linearizing all the graphs from trials 1, it can be observed that a linear relationship exists in the form of $y = mx + b$. The slope, m , is found to be $0.091 \text{ s } T^2$. The best-fit line goes through the error bars of all the data points in trial 3, which has the smallest RSME of 4.0. While the best-fit curves of non-linearized graphs 2, 3, and 4, had negative slopes, the best-fit line of linearized graph 5 has a positive slope. As the inverse of magnetic field strength squared increases, the braking time increased linearly.

It should also be noted that a braking time intercept existed in all graphs, meaning the theoretical proportional relationship between braking time and B_0^{-2} did not exist in these trials.

Evaluation of procedure and results

All trials were graphed on a Braking time vs Magnetic Field Strength graph and the relationship between braking time and the magnetic field strength was found to be governed by the following equation:

$$\Delta t = \frac{A}{B_0^2}$$

A was found to be 0.099.

The relationship between braking time and the inverse square of magnetic field strength was found to be governed by the following equation:

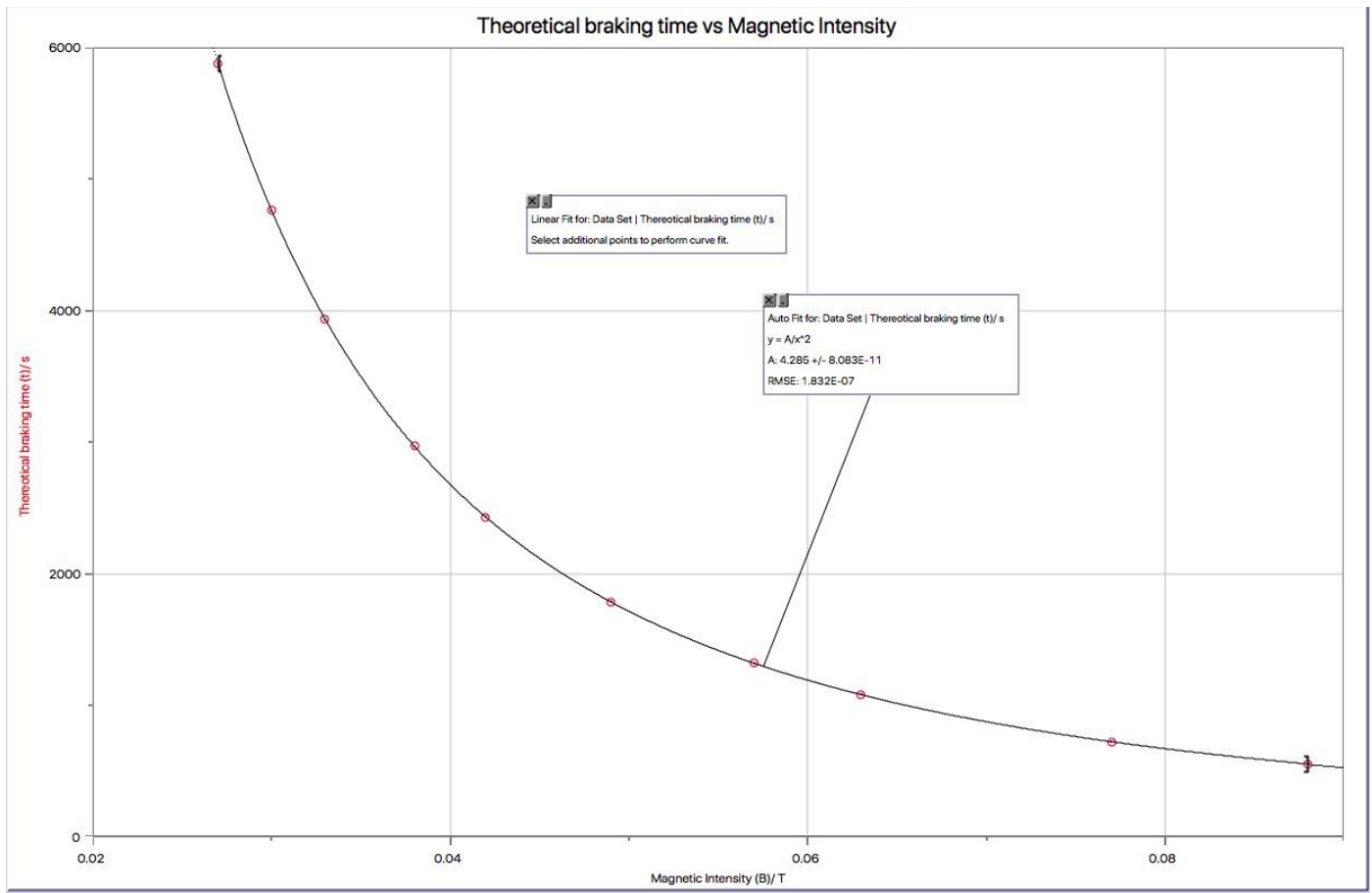
$$y = mx + b$$

m was found to be $0.091 \text{ s } T^2$.

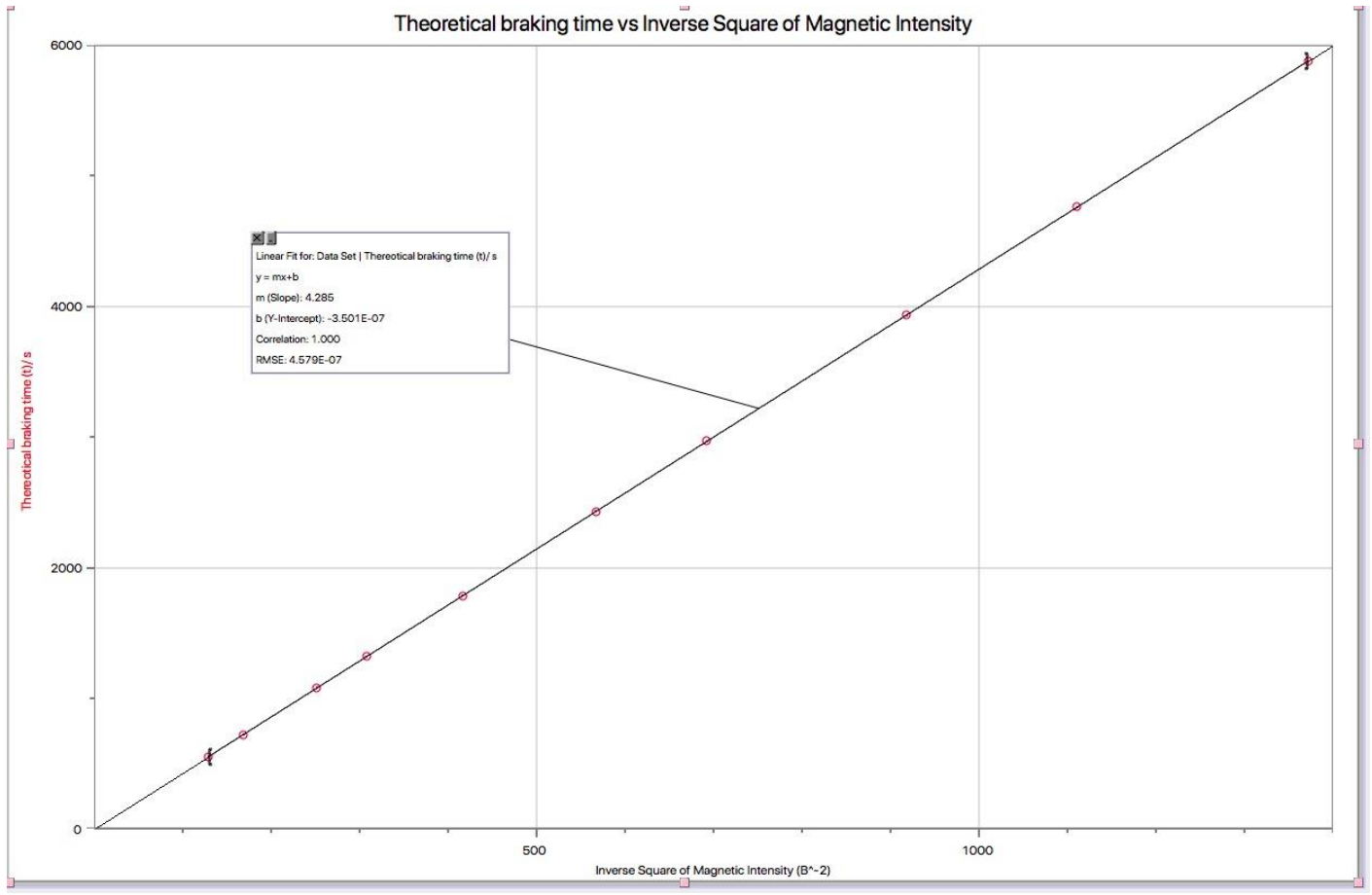
The best-fit curve of Braking time vs Magnetic Field Strength graphs did not model the data perfectly and most graphs had a root mean square error of 5.0 or 6.0, which are very high.

However, when these data points were plotted on a Braking time vs Inverse square of Magnetic Field Strength graph, the best-fit line mirrored the data points better, with most graphs having a RMSE of around 4.0.

The theoretical braking time values can be found at each air gap using the measured parameters. The graph of the theoretical braking time values against the magnetic field strength and is shown below.



Graph 6 Theoretical Braking Time vs Magnetic Field Strength



Graph 7 Theoretical Braking Time vs Inverse Square of Magnetic Field Strength

The A value on graph 6 was found to be 4.29 and the m value on graph 7 was found to be 4.29s T^2 . The theoretical values of A and m are much larger than the experimental values.

Calculating c:

$$\text{Eq. 2 } c = 1 - \frac{1}{4\left(1 + \frac{r}{A}\right)^2 \left(\frac{A-r}{l}\right)^2}$$

$$r = 1.09 \times 10^{-1} \text{m}$$

$$A = 2.53 \times 10^{-1} \text{m}$$

$$l = 5.9 \times 10^{-2} \text{m}$$

$$c = 1 - \frac{1}{4\left(1 + \frac{(1.09 \times 10^{-1})\text{m}}{(2.53 \times 10^{-1})\text{m}}\right)^2 \left(\frac{(2.53 \times 10^{-1})\text{m} - (1.09 \times 10^{-1})\text{m}}{(5.9 \times 10^{-2})\text{m}}\right)^2}$$

$$c = 0.09795(\text{unitless})$$

Sample calculation for Braking Time at 0.012m air gap:

$$\text{Eq.8 } \Delta t = \frac{4\rho m}{\pi l^2 T c} \times B_o^{-2}$$

$$\rho = 2.82 \times 10^{-8} \Omega$$

$$m = 9.8 \times 10^{-2} \text{kg}$$

$$l = 5.9 \times 10^{-2} \text{m}$$

$$T = 4.0 \times 10^{-4} \text{m}$$

$$c = 0.9795 \text{ (unitless)}$$

$$B_o = 0.088$$

$$\Delta t = \frac{4 \times 2.82 \times 10^{-8} \times 9.8 \times 10^{-2}}{\pi(5.9 \times 10^{-2})^2 \times 4.0 \times 10^{-4} \times 0.9795} \times 0.088^{-2}$$

$$\Delta t = 0.33\text{s}$$

The experimental braking time for 0.012m air gap was 17.3s. There are a few possibilities to account for this discrepancy. The greatest ones being air resistance, friction inside the dc motor, and imprecise measurements of the parameters.

Evaluation of apparatus:

The apparatus included two main parts, both of which involved construction hand. The first part is the dc motor with the spinning disk. The structure was relatively stable as heavy-duty tape and zip ties were used to keep the motor in place. A potential source of error arises from the fact that the disk is attached to the shaft of the motor on a slight angle. This means the disk rotated on an angle as well, which changes the air gap between the disk and the magnets.

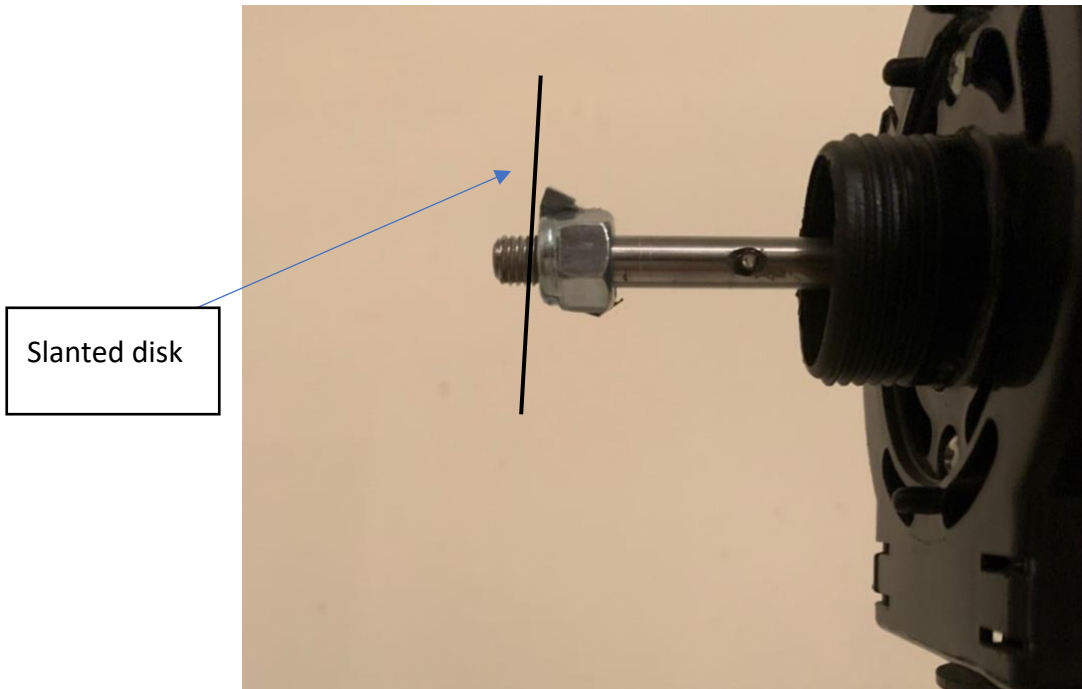


Fig. 16 Close up of the shaft of motor

Additionally, the permanent magnets may have created eddy current within the conductor when it was not supposed to. Magnetic field from magnets are not supposed to interact with disk in the position shown in Fig. 17 but because of the strength of the magnets and the close proximity of the disk to the magnets, the field most likely affects the disk even when the magnets are out of the way.

Fig. 17 Lever machine and disk



Evaluation of results:

These errors in this experiment might seem very large, but there are many contributing factors.

The experimental A and m values are much smaller than the theoretical values.

The skin effect:

This effect describes the phenomenon of electron accumulation in a conductor, which concentrates on the skin or surface of the conducting material. This restricts the generated eddy currents to a small part of the cross-sectional area, increasing the current density in a specific area. The skin effect can possibly have strong effects on the braking torque of the Eddy Current Braking system. This skin effect can increase the conductivity of the conductor and decrease the braking time. This effect becomes more pronounced at high speeds with thicker conductors. A study using a 4mm disk found that when the rotational speed is 150 rpm and below, the generated eddy current stays in the area close to the source of magnetic field, meaning the skin effect is not noticeable⁶. When the rotational speed is increased to 450 rpm, however, the generated current is distributed at the area outside of the magnetic field source, meaning the skin effect is noticeable. In this study, the disk thickness was 0.4mm while the dc motor spun the disk at a speed of 900 rpm. With thinner conductors, such as the one used in this study, the skin effect is negligible. But since the disk in this study was spun at high speeds, the skin effect could possibly have decreased the braking time of the disk in certain trials.

6. Putra, Mufti Reza Aulia, et al. "Application of Multiple Unipolar Axial Eddy Current Brakes for Lightweight Electric Vehicle Braking." *MDPI*, Multidisciplinary Digital Publishing Institute, 6 July 2020,

Human error and external forces

Another major source of error is human error and external forces, such as air resistance. Due to the disk's high speed of rotation, air resistance is inevitable. Additionally, there is friction between the surfaces of different mechanical parts inside the motor itself. Even without the induced eddy current drag, the aluminum disk eventually comes to rest on its own. As long as the external forces play the same role in all the trials a relationship between the variables can still be determined. This requires the experimenter to have coordination and precise timing. If the dc motor is turned off and the magnets are brought into position simultaneously for all trials, then the change in braking time will only be due to the change in air gap. If the dc motor is turned off after the magnets are into proximity, then the disk will already have started slowing down due to external factors and the change in braking time between trials cannot be related to the change in air gap. The experimental process requires high levels of consistency, which is not feasible for a human experimenter.

Conclusion:

In this eddy current braking system, 6 neodymium magnets attached to a simple lever system induces eddy currents in a ferromagnetic disk attached to a dc motor. The independent variable is the air gap between the ferromagnetic aluminum disk and the neodymium magnets. The range for this variable is 0.012m - 0.030m (or 1.20 cm – 3.00 cm), incrementally increasing by 0.002m (0.2cm). The dependent variable is the time it takes the disk to completely stop spinning.

Because the relationship between the magnetic field strength at a particular air gap and braking time were easier to theoretically determine than air gap and braking time, the braking time was plotted against magnetic field strength. Each magnetic field strength corresponded to an air gap; thus, the relationship between braking time and air gap is also determined.

An inverse exponential relationship was found between the braking time of the disk and the magnetic field strength of the neodymium magnets. The theoretical Inverse Squared relationship between braking time and magnetic strength intensity presented at the start of this study was confirmed using experimentally determined data points.

The theoretical braking time values were plotted against magnetic field strength and inverse square of magnetic field strength. The theoretical braking time values were much greater than the experimental braking time values. This may be due to air resistance and internal friction inside the DC motor. As a result, the theoretical graphs have different slope and intercept values compare to the experimental graphs. However, the overall shape and relationship of the theoretical and experimental graphs are the same.

Areas of further research include:

- determining the relationship between initial speed of the disk vs braking time
- determining the effects of air gap on the amount of heat energy produced
- determining the relationship between the area the magnets cover and the braking time

Bibliography

- “(PDF) Application of Multiple Unipolar Axial Eddy Current Brakes for Lightweight Electric Vehicle Braking.” *ResearchGate*,
https://www.researchgate.net/publication/342727635_Application_of_Multiple_Unipolar_Axial_Eddy_Current_Brakes_for_Lightweight_Electric_Vehicle_Braking.
- Chavan, Sneha, et al. “Design and Fabrication of Eddy Current Braking System.” *JETIR*,
JETIR(Www.jetir.org), <https://www.jetir.org/view?paper=JETIRBB06179>.
- Chris Woodford. Last updated: March 23. “How Do Eddy-Current Brakes Work?” *Explain That Stuff*, 23 Mar. 2021, <https://www.explainthatstuff.com/eddy-current-brakes.html>.
- Heald, Mark A. “Magnetic Braking: Improved Theory.” *NASA/ADS*,
<https://ui.adsabs.harvard.edu/abs/1988AmJPh..56..521H/abstract>.
- “How Eddy Current Braking Technology Is Freeing Us from Friction.” *COMSOL*,
<https://www.comsol.com/blogs/how-eddy-current-braking-technology-is-freeing-us-from-friction/>.
- Ma, Der-Ming, and Jaw-Kuen Shiau. “[PDF] the Design of Eddy-Current Magnet Brakes: Semantic Scholar.” *Undefined*, 1 Jan. 1970, <https://www.semanticscholar.org/paper/THE-DESIGN-OF-EDDY-CURRENT-MAGNET-BRAKES-Ma-Shiau/2f7db33ba32714b05ff69ae8b5bb29daeec17eda>.

Oldenburg, Curtis M., et al. "Figure 5. Calculated and Measured Values of Magnetic Field Strength..." *ResearchGate*, 15 Oct. 2020, https://www.researchgate.net/figure/Calculated-and-measured-values-of-magnetic-field-strength-versus-distance-away-from-a_fig5_226151519.

Putra, Mufti Reza Aulia, et al. "Application of Multiple Unipolar Axial Eddy Current Brakes for Lightweight Electric Vehicle Braking." *MDPI*, Multidisciplinary Digital Publishing Institute, 6 July 2020, <https://www.mdpi.com/2076-3417/10/13/4659>.

Shi, Skyler. "(PDF) Investigating the Optimality of a Rotational Eddy Current Brake through Experiments." *ResearchGate*, Unknown, 1 Mar. 2016, https://www.researchgate.net/publication/319310938_Investigating_the_Optimality_of_a_Rotational_Eddy_Current_Brake_through_Experiments.

Shrivastava, Er. Shivanshu. "[PDF] a Parametric Analysis of Magnetic Braking the Eddy Current Brakes for High Speed and Power Automobiles and Locomotives using Simulink: Semantic Scholar." *Undefined*, 1 Jan. 1970, <https://www.semanticscholar.org/paper/A-Parametric-Analysis-of-Magnetic-Braking-The-Eddy-Shrivastava/d46039de9b86bb63f2a293864a3d011260946583>.

Urone, Paul Peter, and Roger Hinrichs. "Eddy Currents and Magnetic Damping." *College Physics*, OpenStax, 23 Jan. 2012, <https://opentextbc.ca/openstaxcollegephysics/chapter/eddy-currents-and-magnetic-damping/>.

Urone, Paul Peter, and Roger Hinrichs. "Eddy Currents and Magnetic Damping." *College Physics*, OpenStax, 23 Jan. 2012,
<https://opentextbc.ca/openstaxcollegephysics/chapter/eddy-currents-and-magnetic-damping/>.

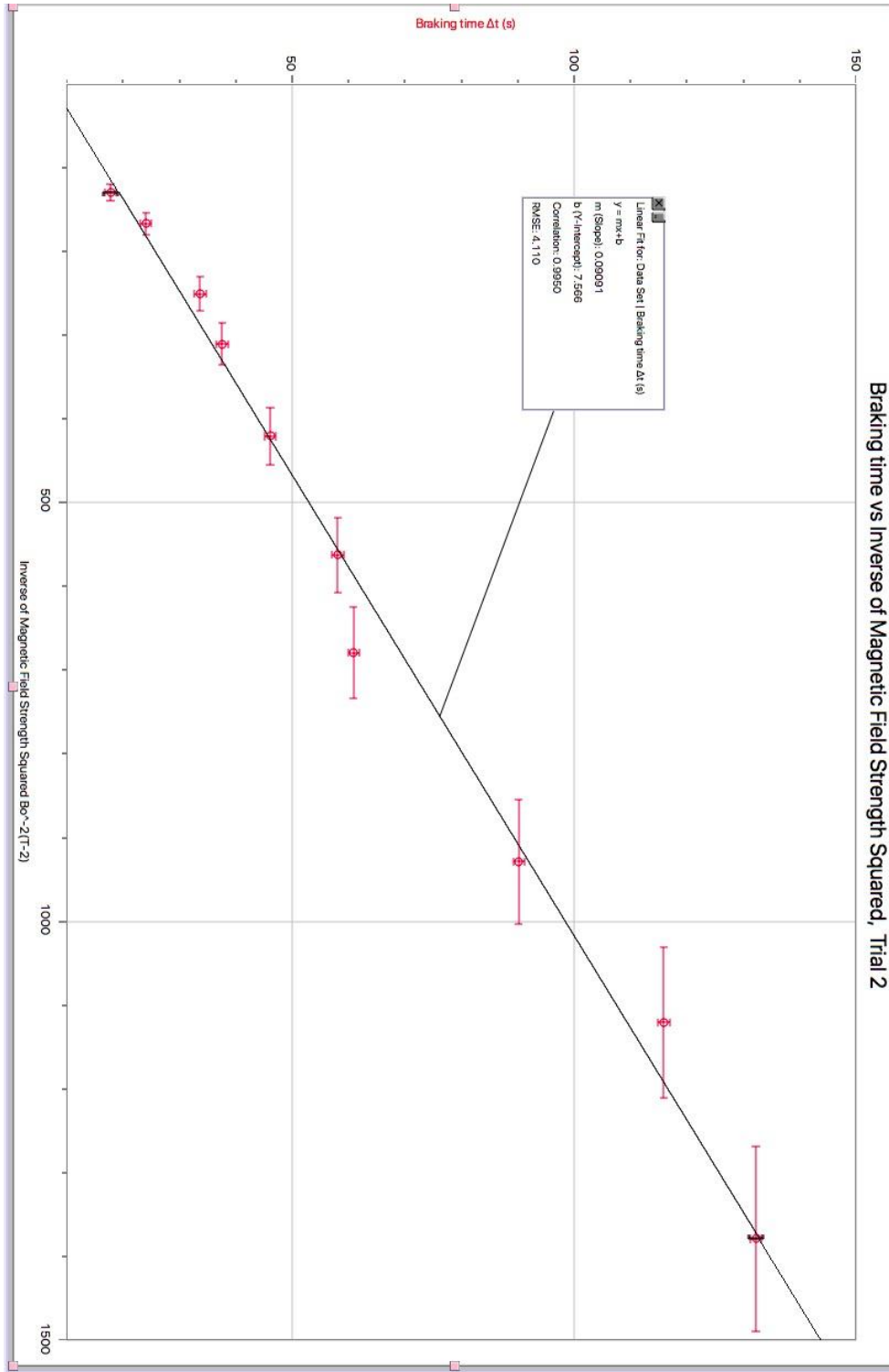
Waloyo, Hery Tri, et al. "A Novel Approach on the Unipolar Axial Type Eddy Current Brake Model Considering the Skin Effect." *MDPI*, Multidisciplinary Digital Publishing Institute, 27 Mar. 2020, <https://www.mdpi.com/1996-1073/13/7/1561>.

"What Is Brake Torque?" *What Is Brake Torque? | Race Technologies | Brembo Official Partner*, <https://www.racetechnologies.com/article/what-brake-torque#:~:text=Brake%20torque%20is%20essentially%20the,system%20equals%20the%20brake%20torque>.

Appendix:

Linearized graphs

Graph 8 Braking time vs Inverse of Magnetic Field Strength Squared, Trial 2



Graph 9 Braking time vs Inverse of Magnetic Field Strength Squared, Trial 3

